

Rectified Iterative Disparity for Stereo Matching

Weiqing Xiao

Abstract

Both uncertainty-assisted and iteration-based methods have achieved great success in stereo matching. However, existing uncertainty estimation methods take a single image and the corresponding disparity as input, which imposes higher demands on the estimation network. In this paper, we propose *Cost volume-based disparity Uncertainty Estimation* (UEC). Based on the rich similarity information in the cost volume coming from the image pairs, the proposed UEC can achieve competitive performance with low computational cost. Secondly, we propose two methods of uncertainty-assisted disparity estimation, *Uncertainty-based Disparity Rectification* (UDR) and *Uncertainty-based Disparity update Conditioning* (UDC). These two methods optimise the disparity update process of the iterative-based approach without adding extra parameters. In addition, we propose *Disparity Rectification loss* that significantly improves the accuracy of small amount of disparity updates. We present a high-performance stereo architecture, *DR Stereo*, which is a combination of the proposed methods. Experimental results from SceneFlow, KITTI, Middlebury 2014, and ETH3D show that DR-Stereo achieves very competitive disparity estimation performance.

Index Terms

3D computer vision, Stereo, Uncertainty, Iteration

I. INTRODUCTION

Depth perception is the basis for computer vision and graphics research in 3D scenes. High-precision depth information is vital for fields such as 3D reconstruction, autonomous driving, and robotics. Stereo matching is an efficient and low-cost depth estimation method that aims at estimating the pixel horizontal displacement map, also known as the disparity map, between the corrected left and right image pairs. Given the camera calibration parameters, we can calculate the depth map from the disparity. In recent years, many learning-based stereo networks [1], [4], [7], [13], [14], [27] have achieved encouraging success in terms of quality and efficiency of disparity estimation. In general, the stereo matching algorithm consists of four steps: matching feature extraction, matching cost computation, cost aggregation and disparity optimization.

Current research in learning-based stereo networks focuses on the quality and efficiency of disparity estimation. 3D convolution-based methods [1], [8], [28] use 3D convolution to aggregate and regularize 4D cost volume,

Weiqing Xiao is with the School of Electronic Information Engineering, Beihang University, Beijing 100191, China, (e-mail: xi-aowqtx@buaa.edu.cn)

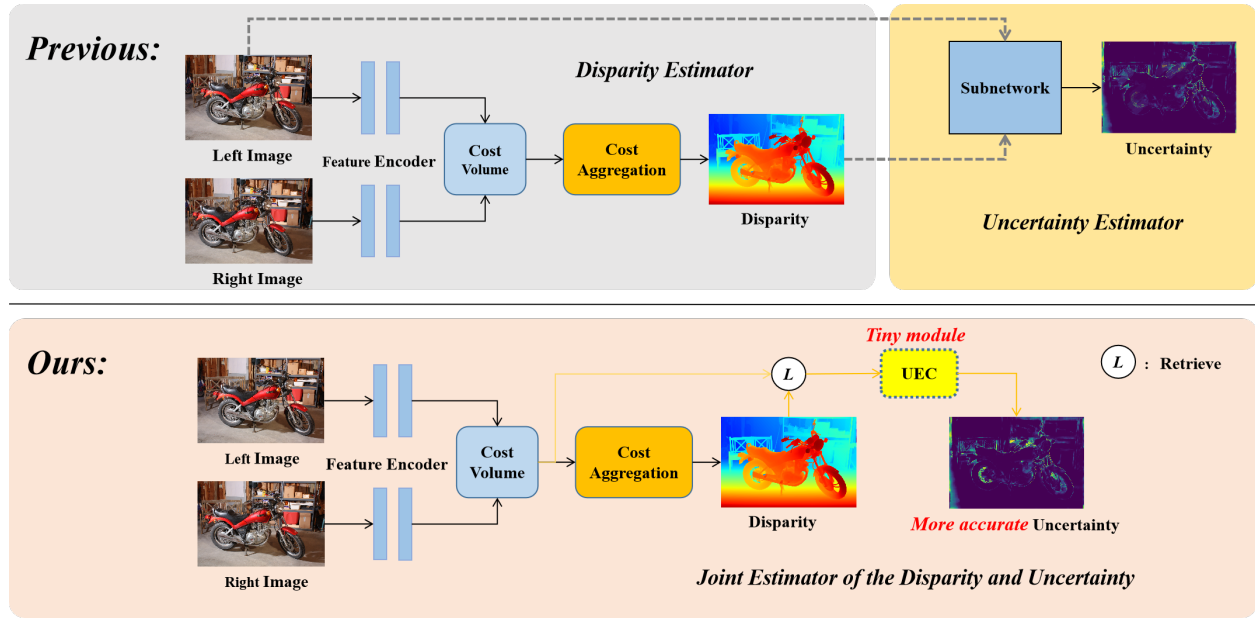


Fig. 1. The cost volume-based disparity uncertainty estimation. This figure compares the architecture between the previous work and ours. The previous work only utilises information from the left image. Our work makes full use of the information in the image pairs and avoids redundant feature extraction steps.

and then regress the disparity map from the regularized cost volume. These methods effectively encode context information as well as stereo geometry information and achieves good performance. However, the cost aggregation and regularization require a large number of 3D convolutions, which limits its practical applicability. Correlation volume-based methods [15], [17], [29], [30] use 2D convolution instead of 3D for cost aggregation, which saves computational cost but also reduces accuracy. Iterative based methods [12], [15], [25], [29], [34] use convolutional GRU [3] or LSTM [6] as the core unit of the update operator to retrieve features from the cost volume and update the disparity map, thus avoiding computationally expensive cost aggregation operations. Such methods have achieved an overall lead in performance and efficiency over other methods and have become the mainstream of research in recent years.

On the other hand, some works [2], [10], [21]–[23] focus on disparity uncertainty estimation, which aims to assist disparity estimation through uncertainty. UCFNet [23] screens the estimated disparity of a new domain based on uncertainty, and uses the screened sparse disparity maps as pseudo-labels to adapt the pre-trained model to the new domain. SEDNet [2] proposes a sub-network to perform the disparity uncertainty estimation, and uses multi-task learning to improve the performance of the disparity estimation network.

Existing studies [2], [22], [23], however, essentially use two completely separate networks to perform disparity uncertainty estimation and disparity estimation, respectively. The uncertainty estimation network takes a single image and the corresponding disparity map as input and directly regresses the uncertainty map. This task-separated approach raises the computational cost and complexity of the overall architecture. Therefore, we investigate the architecture for joint disparity and uncertainty estimation. Inspired by the iteration-based methods [12], [15], [29],

[34], we recognise that the features of the cost-volume indexed by the disparity map contain information about the similarity of the left and right maps under the current disparity in terms of context and local details, which is an important basis for the uncertainty estimation of the disparity map.

In this paper, we propose a new uncertainty estimation method named *Cost volume-based disparity Uncertainty Estimation* (UEC). Based on the rich context and local matching information in the cost volume, UEC accurately performs the disparity uncertainty estimation at a very low computational cost without introducing redundant sub-networks (Fig. 1). In addition, since the construction of the cost volume is a key step in stereo matching, UEC can be inserted into almost all stereo matching methods to efficiently complement the disparity uncertainty information of predicted disparity.

Based on UEC, we propose two new methods for uncertainty-assisted disparity estimation, *Uncertainty-based Disparity Rectification* (UDR) and *Uncertainty-based Disparity update Conditioning* (UDC). The UDR is a lightweight disparity updating unit that updates the disparity by the change in uncertainty after fine-tuning.

The essence of iterative disparity optimisation is the regression of the amount of disparity update on the difference between the current disparity and the ground truth. However, the vast majority of pixel-by-pixel disparity errors during training and inference are within 3 pixels (Table I), i.e., the ideal distribution of disparity updates is a long-tailed distribution. The usual idea to mitigate a long-tailed distribution is to increase the weight of the tail target in the overall loss function, but this does not apply to the amount of disparity updates, for which head accuracy is more important. To solve this problem, UDC splits the large disparity update into several small disparity updates based on the disparity uncertainty. This splitting effectively reduces the regression difficulty of the amount of disparity updates, thus improving the overall accuracy. In addition, the range of the split disparity updates is stable over different domains, which contributes to the generalisation performance of the model.

TABLE I

QUANTITATIVE RESULTS FOR THE DISTRIBUTION OF DISPARITY UPDATES AND THE DISTRIBUTION OF ERRORS. WE PRE-TRAIN IGEV-STEREO ON SCENE FLOW AND CONDUCT EXPERIMENTS DIRECTLY ON THE MIDDLEBURY 2014 TRAINING SET TO STATISTICALLY CHARACTERIZE THE DISTRIBUTION OF THE AMOUNT OF DISPARITY UPDATES AND DISPARITY ERRORS DURING THE ITERATIONS.

Value	$\leq 1px$	$(1px, 3px]$	$(3px, 5px]$	$> 5px$
Updates	97.87%	1.50%	0.28%	0.35%
Errors	83.75%	8.20%	2.48%	5.57%

To further improve the accuracy of small disparity updates, we propose *Disparity Rectification loss* (DR loss). We construct a dynamic weight that increases the focus on pixels with small errors. As the disparity error decreases through iterative updates, the increased accuracy of small disparity updates contributes to the final disparity becoming more accurate. This indicates that DR loss is a more advanced and generalised loss function that generally improves the performance of iteration-based methods. We insert UDR, UDC into the iteration-based method and use DR loss during training. We name this architecture DR-Stereo, for *Disparity Rectification Stereo*.

In summary, our main contributions are:

- A novel uncertainty estimation method, UEC, which efficiently achieves joint estimation of the disparity and uncertainty based on the cost volume.
- Two novel uncertainty-assisted methods for disparity estimation, UDR and UDC. The former performs targeted optimisation of the disparity map through the uncertainty, while the latter effectively mitigates the long-tailed distribution of the amount of disparity updates for the iteration-based methods.
- An advanced and general loss function, DR loss, which increases the focus on small error pixels to improve the accuracy of the final disparity.
- We propose a new stereo method, DR-Stereo, which achieves competitive performance on SceneFlow , KITTI benchmarks, Middlebury 2014 and ETH3D.

II. RELATED WORK

A. Iterative-based Methods

Inspired by the optical flow network RAFT [24], many iterative-based stereo networks [12], [15], [16], [29], [34] have been successful in terms of quality and efficiency of disparity estimation. RAFT-Stereo [15] is the first iterative-based stereo architecture to be proposed. The overall design is based on RAFT [24], replacing the all-pairs of 4D correlation volume with a 3D volume. In addition, it introduces a multilevel GRU unit [3], which remains hidden at multiple resolutions with cross connectivity, but still generates a single high-resolution disparity update. CREStereo [12] designs a hierarchical network with recurrent refinement, updating the disparity in a coarse-to-fine pattern, which leads to a better restoration of fine depth details. DLNR [34] proposes an LSTM-based decoupling module to iteratively update the disparity and allows features containing fine details to be shifted iteratively, mitigating the problem that information can be lost during iteration. IGEV-Stereo [29] constructs a combined geometric encoding volume that encodes geometric and context information as well as local matching details and iteratively indexes them to update the disparity map for optimal performance.

B. Estimation of Disparity Uncertainty

High-performance stereo methods are not error-free, thus it is vital to correlate uncertainty with its estimation. UCFNet [23] uses pixel-level and region-level uncertainty estimation to filter out highly uncertain pixels from the predicted disparity maps and generates sparse and reliable pseudo-labels, which is used to fine-tune the model so that the model applies to new domains. SEDNet [2] proposes a new loss function and an uncertainty estimation subnetwork for joint disparity and uncertainty estimation, which improves the performance of all tasks through multi-task learning. However, all these methods [2], [10], [11], [22], [23] require both the disparity and the original image as inputs to estimate the uncertainty, which leads to inefficiency and redundancy in the overall process. We directly predict the disparity uncertainty by indexing features of the cost volume by the disparity. Our proposed UEC can be integrated into existing stereo methods to efficiently estimate the disparity uncertainty and efficiently achieves joint estimation of the disparity and uncertainty. In addition, by virtue of the low computational cost of UEC, we propose two novel uncertainty-assisted methods for disparity estimation, UDR and UDC, which further improve the performance of disparity estimation.

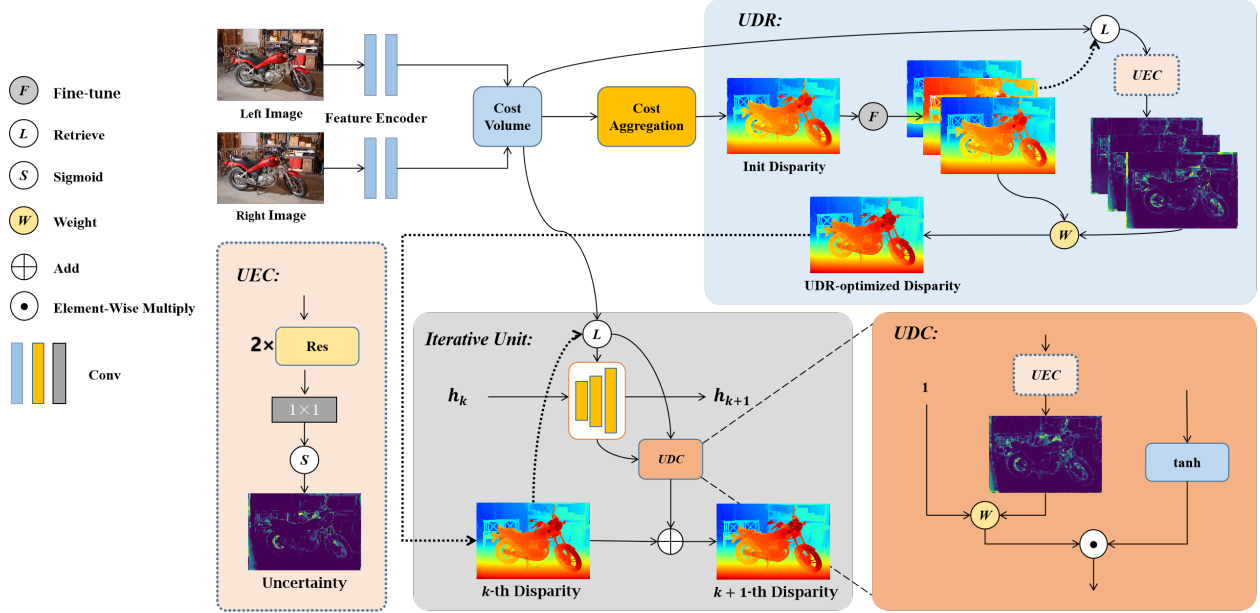


Fig. 2. Overview of our proposed DR-Stereo. We estimate the disparity uncertainty by cost volume. The init disparity is coarsely optimised once in the UDR and then finely optimised several times through the iterative unit. In the iterative unit, the proposed UDC moderates the disparity update to keep the update range stable.

III. METHODS

In Fig. 1, we describe the general process of UEC. In this section, we further demonstrate the feasibility of UEC and describe the specific implementation of UEC. At the same time, we describe the proposed UDR and UDC, and show how to insert them into a general iterative stereo matching network (the overall architecture is shown in Fig. 2). Finally, we propose DR loss to compute the prediction error for each level of disparity.

A. Cost volume-based Disparity Uncertainty Estimation

Feasibility Study: To prove the feasibility of the UEC architecture, we compare the loss function of the iteration-based method with that of the disparity uncertainty estimation. For the former, the loss function can be expressed as:

$$L_{stereo} = \sum_{i=0}^{total_{itr}} \gamma^{total_{itr}-i} \|d_i - d_{gt}\| \quad (1)$$

where d_{gt} is the ground truth disparity, d_i is the disparity of the i -th iteration, $total_{itr}$ is the total number of iterations. In the iteration-based method, d_i is obtained by continuous iterative optimisation of the initial disparity map d_0 :

$$d_i = d_0 + \Delta d_0 + \Delta d_1 + \dots + \Delta d_{i-1} \quad (2)$$

where Δd_{i-1} is the amount of disparity update in the i -th iteration. Therefore, the regression target of the amount of disparity update is essentially the difference $d_{gt} - d_{pred}$ between the ground truth and the current disparity. As

for the disparity uncertainty estimation, existing studies usually obtain the uncertainty ground truth based on the difference between the ground truth of the disparity and the predicted disparity:

$$U_{gt}(d_{pred}) = \begin{cases} 0 & , \quad |d_{gt} - d_{pred}| \leq thr \\ 1 & , \quad otherwise \end{cases} \quad (3)$$

The target of the regression of disparity uncertainty can be regarded as a nonlinear transform of the difference $d_{gt} - d_{pred}$ between the ground truth of the disparity and the current disparity, i.e., a nonlinear transform of the ideal amount of disparity update Δd . Thus estimation of the disparity uncertainty by means of the features indexed by the disparity map to the cost volume is undoubtedly a more reliable and direct way, and this architecture is an efficient implementation of a joint estimation of disparity and uncertainty.

Specific implementation: The iteration-based methods use the current disparity d_k to index features for disparity updating from a two-level C_{volume} pyramid via linear interpolation:

$$G_f(d_k) = \sum_{i=-r}^r Concat \{C_{volume}(d_k + i), C_{volume}^p(d_k/2 + i)\} \quad (4)$$

where r is the index radius and p denotes the pooling operation. Based on the rich similarity information in C_{volume} , the UEC predicts the uncertainty of the current disparity using only the retrieved features $G_f(d_k)$ as inputs:

$$U(d_k) = \sigma(conv_{1 \times 1}(Res(Res(G_f(d_k)))))) \quad (5)$$

where σ is the sigmoid function and Res is the residual block [9]. The UEC can estimate the uncertainty of multiple disparity maps output from the network at a low computational cost.

The uncertainty ground truth : In order to calculate the disparity uncertainty more accurately, we have improved Eq.3. We propose to use the sigmoid function to calculate the ground truth uncertainty:

$$U_{gt}(d_k) = \sigma(a \times |d_{gt} - d_k| - thr) \quad (6)$$

where a is the transition distance between correct to incorrect predictions. As the a tends to infinity, Eq.6 is approximately equivalent to Eq.3. In Section IV-D, we explore the effect of the uncertainty ground truth setting on the accuracy of the uncertainty estimation and find that the best results are obtained with $a = 1.5$ and $thr = 3.0$.

B. Disparity Rectification

In this section, we introduce two uncertainty-assisted methods for disparity estimation, *Uncertainty-based Disparity Rectification* (UDR) and *Uncertainty-based Disparity update Conditioning* (UDC).

Uncertainty-based Disparity Rectification: The disparity uncertainty is related to the magnitude of the expected error. We consider it a beneficial update if the disparity uncertainty is reduced. In *Uncertainty-based Disparity Rectification* (UDR), the disparity map is fine-tuned as a whole and then the uncertainty is recalculated by UEC. The original disparity is updated by combining the recalculated uncertainty with the fine-tuning magnitude:

$$d_{UDR}^{k+1} = d_k + s \times (U(d_k - s) - U(d_k + s)) \quad (7)$$

where s is the fine-tuning magnitude of the disparity map. The UDR is an intuitive and effective method of disparity optimization, and in this paper we use it to optimize the initial disparity map, which has the greatest impact on the disparity performance.

Uncertainty-based Disparity Update Conditioning: The process of updating the disparity for the iterative stereo matching method can be described as follows:

$$h_k = \text{Unit}_{update}(G_f(d_k), h_{k-1}, d_k) \quad (8)$$

$$d_{k+1} = d_k + \text{Decoder}_d(h_k) \quad (9)$$

where Unit_{update} is the disparity update unit, h_k is the current hidden state of the update unit, Decoder_d is the decoder used to output the amount of disparity updates. We propose *Uncertainty-based Disparity update Conditioning* (UDC), which regulates the amount of disparity update through the disparity uncertainty:

$$d_{UDC}^{k+1} = d_k + m \times \tanh\left(\frac{\text{Decoder}_d(h_k)}{m}\right) \odot (1 + 0.5 \times U(d_k)) \quad (10)$$

where m is the modulation factor of the UDC and \odot denotes the Hadamard Product. We control the upper limit of the amount of disparity updates by m , thus splitting the large amount of disparity updates into several smaller ones. In addition, the h_k contains information $\{G_f(d_i)\}_{i=1}^k$ about the previous disparity, providing additional guidance on the disparity update. For pixels with high uncertainty, we encourage larger disparity updates so that the h_k receives more surrounding features.

Notably, the UDC and UDR can be incorporated repeatedly into iteration-based methods at almost negligible cost (see Section IV-D for more details).

C. Disparity Rectification Loss

We observe that in the existing loss functions (e.g., L1 loss and Smooth L1 loss), the effect of pixels decreases as the error decreases, which restricts the upper limit of the accuracy of small disparity updates. Therefore, we propose weights that tend to focus on pixels with small errors:

$$w_{DR}(d_k) = \exp(-\alpha \times |d_k - d_{gt}|) + \beta \quad (11)$$

where α and β are used to control the distribution and the overall scale of weights. It is shown in Section III-D how to combine this weight with L1 loss and Smooth L1 loss. In this paper, we set α to 1/8 and β to 1/10, and demonstrate its validity experimentally (see Section IV-D and IV-F for more details).

D. Loss Function

We calculate the smooth L1 loss on the initial disparity d_0 and the UDR-optimized disparity d_{UDR}^1 and weight them using their rectification weights:

$$L_{init} = w_{DR}(d_0) \odot \text{Smooth}_{L_1}(d_0 - d_{gt}) \quad (12)$$

$$L_{UDR} = w_{DR}(d_{UDR}^1) \odot \text{Smooth}_{L_1}(d_{UDR}^1 - d_{gt}) \quad (13)$$

We calculate the L1 loss on all predicted disparities $\{d_{UDC}^i\}_{i=1}^{total_{itr}}$ and jointly weight them using exponentially increasing weights and rectification weights:

$$L_{UDC} = \sum_{i=1}^{total_{itr}} \gamma^{total_{itr}-i} \times w_{DR}(d_{UDC}^i) \odot \|d_{UDC}^i - d_{gt}\| \quad (14)$$

where $\gamma = 0.9$. We calculate the smooth L1 loss on all disparity uncertainties:

$$L_{UEC}(d_{UDC}^i) = Smooth_{L_1}(U(d_{UDC}^i) - U_{gt}(d_{UDC}^i)) \quad (15)$$

The total loss is defined as:

$$L_{total} = L_{init} + L_{UDR} + L_{UDC} + \sum_{i=1}^{total_{itr}} L_{UEC}(d_{UDC}^i) \quad (16)$$

IV. EXPERIMENTS

A. DATASETS

Scene Flow [17] is a synthetic dataset containing 35,454 training pairs and 4,370 test pairs, and we use Finalpass of Scene Flow because it is closer to real-world images. **KITTI 2012** [5] and **KITTI 2015** [18] are datasets of real-world driving scenes. KITTI 2012 contains 194 training pairs and 195 test pairs, while KITTI 2015 contains 200 training pairs and 200 test pairs. Both KITTI datasets provide sparse ground truth disparities obtained using LiDAR. **Middlebury 2014** [19] is an indoor dataset that provides 15 training pairs and 15 test pairs, with some of the samples being inconsistent under lighting or color conditions. **ETH3D** [20] contains a variety of indoor and outdoor scenes, and provides 27 training pairs and 20 test pairs.

B. Implementation Details

The framework is implemented using PyTorch and We used NVIDIA RTX 3090 GPUs for our experiments. On Scene Flow, the final model is trained with a batch size of 8 for a total of 200k steps, while the ablation experiments are trained with a batch size of 4 for 50k steps. On KITTI, we finetune the pre-trained sceneflow model on a mixed KITTI 2012 and KITTI 2015 training image pair for 50k steps. The ablation experiments are trained using 10 update iterations during training, and the final model is trained using 22 update iterations. The final model and the ablation experiments use a one-cycle learning rate schedule with a learning rate of 0.0002 and 0.0001, respectively. We demonstrate the generalization performance of our method by testing the pre-trained Scene Flow model directly on the training sets of Middlebury 2014 and ETH3D.

C. Estimation of Disparity Uncertainty

In this section, we compare the uncertainty estimation performance between the UEC architecture and the task-separated architecture for the same number of parameters and explore the impact of the ground truth setting. To confirm the generality of the UEC architecture, we conducted experiments with several common cost volumes. Comparing (a) and others in Table II, the uncertainty estimation performance of our proposed UEC architectures generally outperforms that of task-separated architectures. Among all experiments of UEC architectures, the combined volume Gwc8-Cat8 achieves the best overall performance, while Correlation performs relatively poorly due to the loss of

TABLE II

QUANTITATIVE RESULTS OF UNCERTAINTY ESTIMATION ON THE SCENEFLOW TEST SET. IN ADDITION TO USING THE AREA UNDER THE ROC CURVE (AUC), WE PROPOSE PER-PIXEL UNCERTAINTY ERROR (PUE) TO QUANTITATIVELY EVALUATE UNCERTAINTY ESTIMATION PERFORMANCE. GWC REFERS TO GROUP-WISE CORRELATION VOLUME, AND CAT STANDS FOR CONCATENATION VOLUME. **BOLD**: BEST.

	Input	a	thr	AUC↓	PUE↓		Input	a	thr	AUC↓	PUE↓
(a)	$Image_{left} + Disp$	1.5	3.0	0.155	0.061	(f)	Gwc8	1000.0	2.0	0.150	0.044
(b)	Correlation	1.5	3.0	0.154	0.059	(g)	Gwc8	1.0	4.0	0.146	0.041
(c)	Cat8	1.5	3.0	0.147	0.048	(h)	Gwc8	2.0	2.0	0.142	0.062
(d)	Cat16	1.5	3.0	0.133	0.045	(i)	Gwc8	1.5	3.0	0.144	0.047
(e)	Gwc8-Cat8	1.5	3.0	0.133	0.044	(j)	Gwc16	1.5	3.0	0.135	0.046

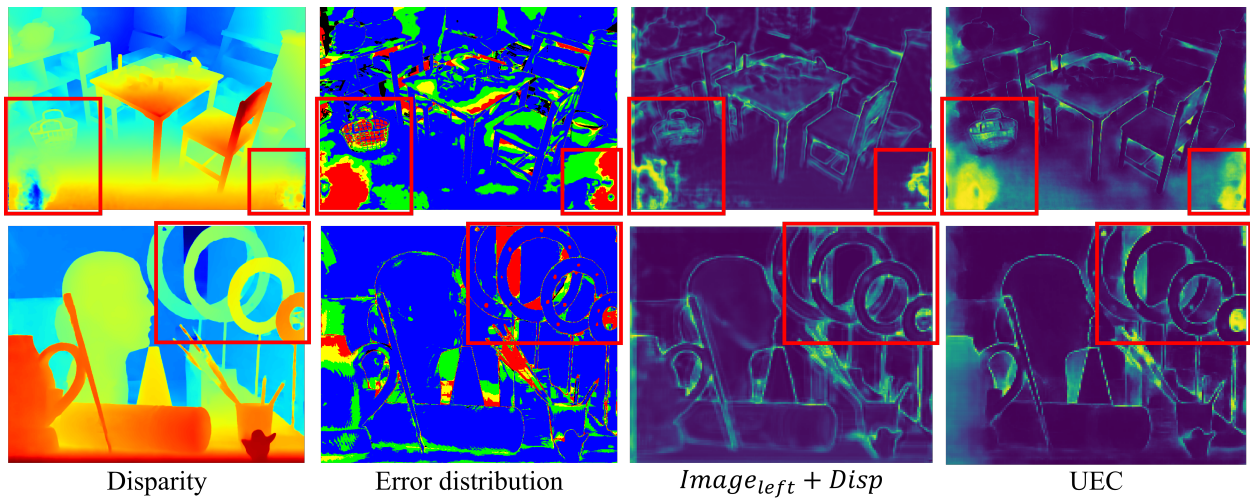


Fig. 3. The qualitative results of UEC on Middlebury 2014. The error distribution of disparity is plotted with the largest error in the red region and the smallest error in the blue region. We pre-train our model on Scene Flow and test it directly on Middlebury 2014. On the new domain, the sensitivity of UEC to disparity error is superior to that of task-separated architectures.

too much information during the construction process (but still approximates the task-separated architecture). In Table II, the improvement from (c) to (d) and from (i) to (j) is significant, which indicates that richer similarity information is beneficial for uncertainty estimation. This further exemplifies the commonality between uncertainty estimation and disparity estimation in terms of required features. In addition, with smoother ground truth settings ((f)~(i)), the UEC achieves an overall improvement on the uncertainty estimation performance. Fig. 3 shows the qualitative results of the two uncertainty estimation architectures at Middlebury 2014. The proposed UEC significantly outperforms the previous architecture in terms of generalisation for disparity uncertainty estimation and performs well in the object edge region.

TABLE III

ABLATION STUDY OF DISPARITY RECTIFICATION. THE BASELINE IS IGEV-STEREO. ALL MODELS ARE TRAINED ON SCENE FLOW. THE FINAL CONFIGURATION OF THE UDC AND UDR IS UNDERLINED. **BOLD**: BEST.

Methods	Variations	Scene Flow		Middlebury-H		ETH3D	
		EPE(px)	> 3px(%)	EPE(px)	> 2px(%)	EPE(px)	> 1px(%)
Baseline	-	0.72	3.65	1.28	8.44	0.492	4.49
+ UDC	<u>$m = 2$</u>	0.69	3.54	1.14	8.05	0.421	4.15
	$m = 3$	0.70	3.58	1.12	7.55	0.467	4.59
	$m = 4$	0.69	3.52	1.32	7.98	0.474	4.54
+ UDR	$s = 2.0$	0.71	3.59	1.08	7.69	0.486	4.44
	<u>$s = 3.0$</u>	0.71	3.57	1.08	7.37	0.479	4.40

D. Ablation Study

Configuration Exploration: We explore the optimal configuration of the proposed method. Table III shows the results of UDR and UDC with different configurations. In the vast majority of cases, UDR and UDC outperform the baseline on several datasets. We argue that the disparity distributions on different datasets are very variable, which makes it difficult to generalise the method trained under a fixed range of disparities to another dataset. However, the range of uncertainty is stable. Therefore, UDR and UDC are two beneficial complements, especially for the exploitation of uncertainty information, which significantly improves the generalisation performance of the model. In addition, to demonstrate the generality of the proposed DR loss over different iteration-based methods, we conduct experiments in both RAFT-Stereo and IGEV-Stereo. As shown in Table IX, both methods achieve improvements on $D1_{error}$ for all configurations of DR loss. Notice that when β is changed from 0.5 to 0.1, the rectification weights are decreased as a whole, but $D1_{error}$ is optimally improved. This phenomenon demonstrates the focus of DR loss on small error pixels, especially when the weights are more skewed.

Combinations of proposed methods: As shown in Table V, we experiment with multiple combinations of the proposed methods. Comparing the results with those in Tables III and IX, our methods achieve further improvements after combination. In addition, we record the increase in the number of parameters, time consumption after inserting the design modules. It can be seen that inserting the UDR and UDC puts little burden for the model. As we present in Section III-B, the combination of UDR and UDC does not increase the number of parameters compared to a single method, since they share parameters from the UEC module.

E. Update on Bad Initial Disparity

In this section, we investigate the role of UDC in regulating the process of disparity update. The disparity distributions of different datasets tend to be highly different, which leads to large initial disparity errors (i.e., the amount of ideal disparity update) on new domains for iteration-based methods. Our proposed UDC splits the large disparity update into several small disparity updates, which alleviates the difference in the distribution of ideal

TABLE IV

ABLATION STUDY OF DR LOSS. ALL MODELS ARE TRAINED ON SCENE FLOW. THE FINAL CONFIGURATION OF THE DR LOSS IS UNDERLINED. **BOLD**: BEST.

Methods	α	β	Scene Flow		Middlebury-H		ETH3D	
			EPE(px)	> 3px(%)	EPE(px)	> 2px(%)	EPE(px)	> 1px(%)
RAFT-Stereo (R.)	-	-	0.79	4.25	1.98	14.67	0.40	5.24
R. + DR loss	<u>0.125</u>	<u>0.1</u>	0.82	3.61	2.21	11.30	0.34	3.61
	0.125	0.5	0.77	3.91	1.88	12.51	0.36	4.13
	0.250	0.5	0.77	4.04	1.96	13.00	0.32	4.27
IGEV-Stereo (I.)	-	-	0.72	3.65	1.28	8.44	0.50	4.49
I. + DR loss	<u>0.125</u>	<u>0.1</u>	0.80	3.26	1.20	7.47	0.50	3.99
	0.125	0.5	0.71	3.37	1.27	7.79	0.50	4.11
	0.250	0.5	0.72	3.56	1.21	7.92	0.48	3.97

TABLE V

ABLATION STUDY AND COMPLEXITY OF DR-STEREO. THE BASELINE IS IGEV-STEREO. THE LAST TWO COLUMNS ARE THE RESULTS WHEN THE SIZE OF INPUT IMAGE IS 1248×384 . **BOLD**: BEST.

Methods	Scene Flow	Middlebury-H	ETH3D	Params(M)	Time(s)
Baseline	3.65	8.44	4.49	12.60	0.155
UDC (C.) + DR loss	3.37	6.98	4.35	12.77	0.158
UDR (R.) + DR loss	3.34	6.64	4.05	12.77	0.160
C.+R.+DR loss (DR-Stereo)	3.33	6.39	3.99	12.77	0.161

disparity updates between different domains. Fig. 5 shows the effect of UDC on the disparity update process in extreme cases. In regions with large initial disparity errors, the method using UDC performs a faster stepwise optimisation of the disparity and generates a more accurate disparity with the same number of iterations.

F. Benchmarks

In this section, we compare DR-Stereo with the state-of-the-art methods published on Scene Flow and KITTI. Tables VI shows the quantitative results. With similar training strategies, DR-Stereo achieves a new SOTA EPE on the Scene Flow test set. Evaluation results on the KITTI benchmark show that DR-Stereo achieves the best performance on the vast majority of metrics. At the time of writing, our method outperforms all published methods on the online KITTI 2015 leaderboard.

G. Zero-shot Generalization

We pre-train DR-Stereo on Scene Flow and test it directly on Middlebury 2014 and ETH3D. As shown in Table VII, Our DR-Stereo achieves very competitive generalisation performance. Compared with the original optimal

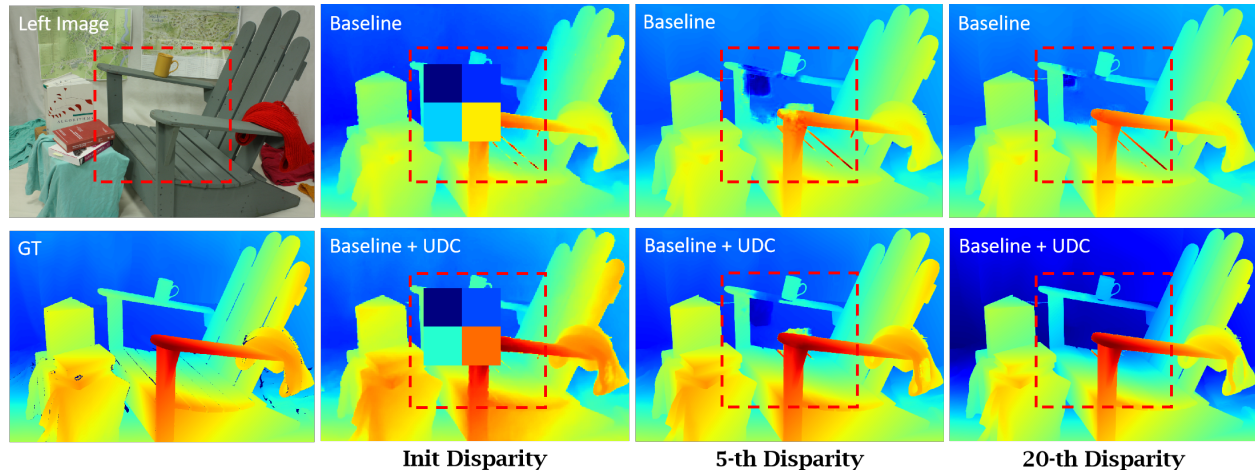


Fig. 4. The effect of UDC in the disparity update process. We mosaic over the initial disparity to simulate the disparity update process in extreme cases. Test image from Middlebury 2014. The baseline is IGEV-Stereo.

TABLE VI
QUANTITATIVE EVALUATION ON SCENE FLOW AND KITTI 2015. **BOLD: BEST.**

Method	Scene Flow	KITTI 2015		
		D1-bg	D1-fg	D1-all
CREStereo [12]	-	1.45	2.86	1.69
DLNR [34]	0.48	1.37	2.59	1.76
Croco-Stereo [26]	-	1.38	2.65	1.59
UPFNet [23]	-	1.38	2.85	1.62
PSMNet [1]	1.09	1.86	4.62	2.32
GANNet [31]	0.80	1.48	3.46	1.81
GwcNet [8]	0.98	1.74	3.93	2.11
AcfNet [33]	0.87	1.51	3.80	1.89
ACVNet [28]	0.48	1.37	3.07	1.65
RAFT-Stereo [15]	0.56	1.58	3.05	1.82
IGEV-Stereo [29]	0.47	1.38	2.67	1.59
DR-Stereo(ours)	0.45	1.37	2.50	1.56

method IGEV-Stereo, our method achieves an overall improvement.

V. CONCLUSION

In this paper, we propose *Cost volume-based disparity Uncertainty Estimation* (UEC). Based on the rich feature information in the cost volume, UEC accurately estimates the disparity uncertainty with very low computational cost. On this basis, we propose *Uncertainty-based Disparity Rectification* (UDR) and *Uncertainty-based Disparity update Conditioning* (UDC). These two methods significantly improve the generalisation performance of the iteration-based methods. We propose the *Disparity Rectification loss* (DR loss), which improves the accuracy of the small amount

TABLE VII

SYNTHETIC DATA GENERALIZATION EXPERIMENTS. WE PRE-TRAIN OUR MODEL ON SCENE FLOW AND TEST IT DIRECTLY ON MIDDLEBURY 2014 AND ETH3D. THE 2-PIXEL ERROR RATE IS USED FOR MIDDLEBURY 2014, AND 1-PIXEL ERROR RATE FOR ETH3D.

BOLD: BEST.

Method	Middlebury		ETH3D	Method	Middlebury		ETH3D
	half	quarter			half	quarter	
PSMNet [1]	15.8	9.8	10.2	CFNet [22]	15.3	9.8	5.8
GANNet [31]	13.5	8.5	6.5	RAFT-Stereo [15]	8.7	7.3	3.2
DSMNet [32]	13.8	8.1	6.2	IGEV-Stereo [29]	7.1	6.2	3.6
STTR [13]	15.5	9.7	17.2	DR-Stereo(ours)	5.5	5.2	3.5

TABLE VIII

QUANTITATIVE RESULTS FOR A SINGLE UDR MODULE. WE RECORD THE RESULTS OF THE UDR UPDATING OF THE INITIAL DISPARITY ON MULTIPLE DATASETS.

Experiment	Scene Flow		Middlebury-H		ETH3D	
	EPE(px)	> 3px(%)	EPE(px)	> 2px(%)	EPE(px)	> 1px(%)
Init disparity	1.04	4.96	1.60	11.87	0.76	10.38
+ UDR	0.98	4.77	1.51	11.01	0.72	9.56

of disparity updates. This improvement contributes to the final disparity becoming more accurate. Finally, we insert UDR, UDC, and DR loss into the iteration-based method and name this new method *Disparity Rectification Stereo* (DR-Stereo). DR-Stereo achieves competitive performance on several publicly available datasets.

VI. MORE RESULTS OF UDR

In DR-Stereo, we update the initial disparity map using the UDR module, which efficiently corrects for obvious disparity errors. Table VIII shows the quantitative results.

VII. PRINCIPLE OF UDC

The UDC splits large disparity updates, thus mitigating the imbalance in the distribution of the ideal amount of updates between different datasets. Fig 5 visualises the impact of the splitting process.

VIII. OTHER ATTEMPTS OF DR LOSS

In this section, we explore alternative forms of DR loss. DRloss is a loss function that focuses on small disparity updates. Table IX shows the many forms we have experimented with. We observe that its specific forms can be varied. While the sigmoid form of DR loss achieves more performance gains, we find experimentally that it is difficult to train when the weight bias is small. Therefore, we did not adopt this setting in the end. We will investigate more possibilities of DR loss in the future.

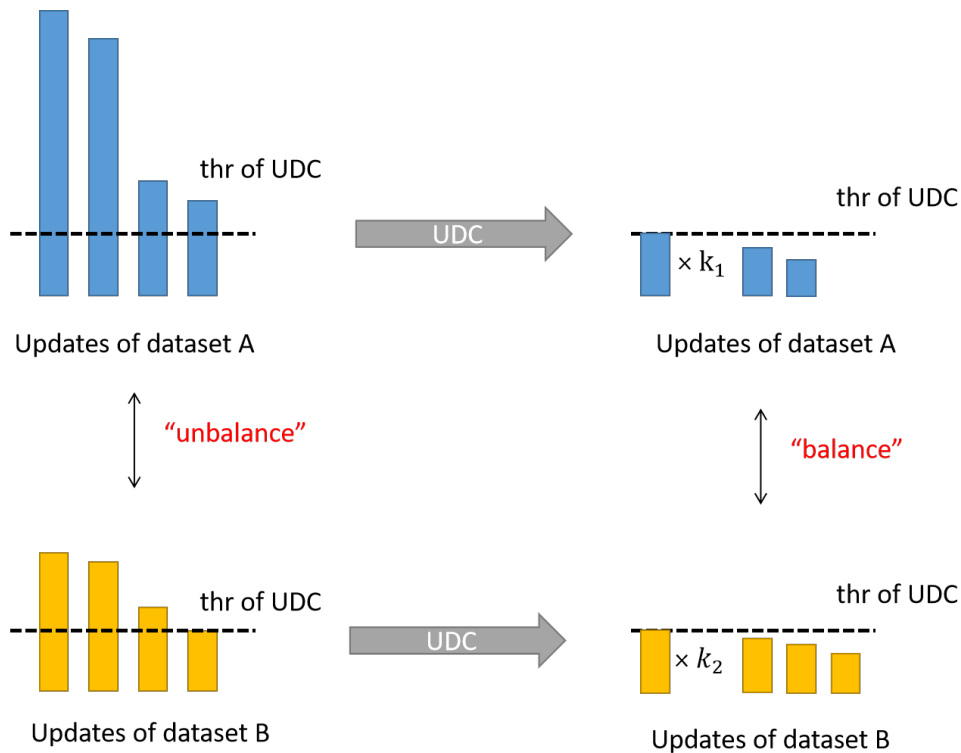


Fig. 5. Splitting process of UDC on different datasets.

TABLE IX
OTHER ATTEMPTS OF DR LOSS. THE BASELINE IS IGEV-STEREO.

Methods	Scene Flow		Middlebury-H		ETH3D
	EPE(px)	$> 3px(\%)$	EPE(px)	$> 2px(\%)$	$> 1px(\%)$
baseline	0.72	3.65	1.28	8.44	4.49
$\exp(-0.125 \times d_k - d_{gt}) + 0.1$	0.80	3.26	1.20	7.47	3.99
$\exp(-0.125 \times d_k - d_{gt}) + 0.5$	0.71	3.37	1.27	7.79	4.11
$\text{sigmoid}(6 - 0.1 \times d_k - d_{gt}) + 0.1$	0.72	3.43	1.16	7.30	3.89
$\text{sigmoid}(6 - 0.5 \times d_k - d_{gt}) + 0.1$	0.72	3.25	1.25	8.00	3.88

REFERENCES

- [1] Chang, J.R., Chen, Y.S.: Pyramid stereo matching network. In: Proceedings of the IEEE conference on computer vision and pattern recognition. pp. 5410–5418 (2018)
- [2] Chen, L., Wang, W., Mordohai, P.: Learning the distribution of errors in stereo matching for joint disparity and uncertainty estimation. In: Proceedings of the IEEE/CVF Conference on Computer Vision and Pattern Recognition. pp. 17235–17244 (2023)
- [3] Cho, K., Van Merriënboer, B., Gulcehre, C., Bahdanau, D., Bougares, F., Schwenk, H., Bengio, Y.: Learning phrase representations using rnn encoder-decoder for statistical machine translation. arXiv preprint arXiv:1406.1078 (2014)
- [4] Duggal, S., Wang, S., Ma, W.C., Hu, R., Urtasun, R.: Deeppruner: Learning efficient stereo matching via differentiable patchmatch. In: Proceedings of the IEEE/CVF international conference on computer vision. pp. 4384–4393 (2019)

- [5] Geiger, A., Lenz, P., Urtasun, R.: Are we ready for autonomous driving? the kitti vision benchmark suite. In: 2012 IEEE conference on computer vision and pattern recognition. pp. 3354–3361. IEEE (2012)
- [6] Graves, A., Graves, A.: Long short-term memory. Supervised sequence labelling with recurrent neural networks pp. 37–45 (2012)
- [7] Gu, X., Fan, Z., Zhu, S., Dai, Z., Tan, F., Tan, P.: Cascade cost volume for high-resolution multi-view stereo and stereo matching. In: Proceedings of the IEEE/CVF conference on computer vision and pattern recognition. pp. 2495–2504 (2020)
- [8] Guo, X., Yang, K., Yang, W., Wang, X., Li, H.: Group-wise correlation stereo network. In: Proceedings of the IEEE/CVF conference on computer vision and pattern recognition. pp. 3273–3282 (2019)
- [9] He, K., Zhang, X., Ren, S., Sun, J.: Deep residual learning for image recognition. In: Proceedings of the IEEE conference on computer vision and pattern recognition. pp. 770–778 (2016)
- [10] Kim, S., Min, D., Kim, S., Sohn, K.: Unified confidence estimation networks for robust stereo matching. *IEEE Transactions on Image Processing* **28**(3), 1299–1313 (2018)
- [11] Kim, S., Min, D., Kim, S., Sohn, K.: Adversarial confidence estimation networks for robust stereo matching. *IEEE Transactions on Intelligent Transportation Systems* **22**(11), 6875–6889 (2020)
- [12] Li, J., Wang, P., Xiong, P., Cai, T., Yan, Z., Yang, L., Liu, J., Fan, H., Liu, S.: Practical stereo matching via cascaded recurrent network with adaptive correlation. In: Proceedings of the IEEE/CVF conference on computer vision and pattern recognition. pp. 16263–16272 (2022)
- [13] Li, Z., Liu, X., Drenkow, N., Ding, A., Creighton, F.X., Taylor, R.H., Unberath, M.: Revisiting stereo depth estimation from a sequence-to-sequence perspective with transformers. In: Proceedings of the IEEE/CVF international conference on computer vision. pp. 6197–6206 (2021)
- [14] Liang, Z., Guo, Y., Feng, Y., Chen, W., Qiao, L., Zhou, L., Zhang, J., Liu, H.: Stereo matching using multi-level cost volume and multi-scale feature constancy. *IEEE transactions on pattern analysis and machine intelligence* **43**(1), 300–315 (2019)
- [15] Lipson, L., Teed, Z., Deng, J.: Raft-stereo: Multilevel recurrent field transforms for stereo matching. In: 2021 International Conference on 3D Vision (3DV). pp. 218–227. IEEE (2021)
- [16] Ma, Z., Teed, Z., Deng, J.: Multiview stereo with cascaded epipolar raft. In: European Conference on Computer Vision. pp. 734–750. Springer (2022)
- [17] Mayer, N., Ilg, E., Hausser, P., Fischer, P., Cremers, D., Dosovitskiy, A., Brox, T.: A large dataset to train convolutional networks for disparity, optical flow, and scene flow estimation. In: Proceedings of the IEEE conference on computer vision and pattern recognition. pp. 4040–4048 (2016)
- [18] Menze, M., Geiger, A.: Object scene flow for autonomous vehicles. In: Proceedings of the IEEE conference on computer vision and pattern recognition. pp. 3061–3070 (2015)
- [19] Scharstein, D., Hirschmüller, H., Kitajima, Y., Krathwohl, G., Nešić, N., Wang, X., Westling, P.: High-resolution stereo datasets with subpixel-accurate ground truth. In: Pattern Recognition: 36th German Conference, GCPR 2014, Münster, Germany, September 2-5, 2014, Proceedings 36. pp. 31–42. Springer (2014)
- [20] Schops, T., Schonberger, J.L., Galliani, S., Sattler, T., Schindler, K., Pollefeys, M., Geiger, A.: A multi-view stereo benchmark with high-resolution images and multi-camera videos. In: Proceedings of the IEEE conference on computer vision and pattern recognition. pp. 3260–3269 (2017)
- [21] Shaked, A., Wolf, L.: Improved stereo matching with constant highway networks and reflective confidence learning. In: Proceedings of the IEEE conference on computer vision and pattern recognition. pp. 4641–4650 (2017)
- [22] Shen, Z., Dai, Y., Rao, Z.: Cfnet: Cascade and fused cost volume for robust stereo matching. In: Proceedings of the IEEE/CVF Conference on Computer Vision and Pattern Recognition. pp. 13906–13915 (2021)
- [23] Shen, Z., Song, X., Dai, Y., Zhou, D., Rao, Z., Zhang, L.: Digging into uncertainty-based pseudo-label for robust stereo matching. *IEEE Transactions on Pattern Analysis and Machine Intelligence* (2023)
- [24] Teed, Z., Deng, J.: Raft: Recurrent all-pairs field transforms for optical flow. In: Computer Vision–ECCV 2020: 16th European Conference, Glasgow, UK, August 23–28, 2020, Proceedings, Part II 16. pp. 402–419. Springer (2020)
- [25] Wang, H., Fan, R., Cai, P., Liu, M.: Pvstereo: Pyramid voting module for end-to-end self-supervised stereo matching. *IEEE Robotics and Automation Letters* **6**(3), 4353–4360 (2021)
- [26] Weinzaepfel, P., Lucas, T., Leroy, V., Cabon, Y., Arora, V., Brégier, R., Csurka, G., Antsfeld, L., Chidlovskii, B., Revaud, J.: Croco v2: Improved cross-view completion pre-training for stereo matching and optical flow. In: Proceedings of the IEEE/CVF International Conference on Computer Vision. pp. 17969–17980 (2023)

- [27] Xu, B., Xu, Y., Yang, X., Jia, W., Guo, Y.: Bilateral grid learning for stereo matching networks. In: Proceedings of the IEEE/CVF Conference on Computer Vision and Pattern Recognition. pp. 12497–12506 (2021)
- [28] Xu, G., Cheng, J., Guo, P., Yang, X.: Attention concatenation volume for accurate and efficient stereo matching. In: Proceedings of the IEEE/CVF Conference on Computer Vision and Pattern Recognition. pp. 12981–12990 (2022)
- [29] Xu, G., Wang, X., Ding, X., Yang, X.: Iterative geometry encoding volume for stereo matching. In: Proceedings of the IEEE/CVF Conference on Computer Vision and Pattern Recognition. pp. 21919–21928 (2023)
- [30] Yang, G., Zhao, H., Shi, J., Deng, Z., Jia, J.: Segstereo: Exploiting semantic information for disparity estimation. In: Proceedings of the European conference on computer vision (ECCV). pp. 636–651 (2018)
- [31] Zhang, F., Prisacariu, V., Yang, R., Torr, P.H.: Ga-net: Guided aggregation net for end-to-end stereo matching. In: Proceedings of the IEEE/CVF Conference on Computer Vision and Pattern Recognition. pp. 185–194 (2019)
- [32] Zhang, F., Qi, X., Yang, R., Prisacariu, V., Wah, B., Torr, P.: Domain-invariant stereo matching networks. In: Computer Vision–ECCV 2020: 16th European Conference, Glasgow, UK, August 23–28, 2020, Proceedings, Part II 16. pp. 420–439. Springer (2020)
- [33] Zhang, Y., Chen, Y., Bai, X., Yu, S., Yu, K., Li, Z., Yang, K.: Adaptive unimodal cost volume filtering for deep stereo matching. In: Proceedings of the AAAI Conference on Artificial Intelligence. vol. 34, pp. 12926–12934 (2020)
- [34] Zhao, H., Zhou, H., Zhang, Y., Chen, J., Yang, Y., Zhao, Y.: High-frequency stereo matching network. In: Proceedings of the IEEE/CVF Conference on Computer Vision and Pattern Recognition. pp. 1327–1336 (2023)

Weiqing Xiao received the B.S. degree from SHENYUAN Honors College of Beihang University in 2022. He is currently pursuing the master's degree in School of Electronic Information Engineering, Beihang University. His research interests include computer vision and 3D vision.